## SURFACE ENERGY

Atoms at a surface or interface are in an environment that is markedly different from the environment of atoms in the bulk of the solid. They may be surrounded by fewer neighbors and these neighbors may be more anisotropic than in the bulk. Thus, we need to be able to quantify the excess properties of surfaces and interfaces.

This part begins by defining some of the basic thermodynamic quantities that we need to discuss surfaces. It then shows that there is a strong correlation between the surface energies of solids and liquids with certain bulk properties, which depend directly on the interatomic potential developed in Part I. This leads naturally to a discussion of nearest-neighbor bond models of surfaces and surface energy, which are followed by surface anisotropy and real atomistic models of surfaces. We then develop a thermodynamic treatment of surfaces in order to quantify phenomena such as segregation and adsorption to surfaces and interfaces.

## 3.1. DEFINITION OF SURFACE ENERGY AND THERMODYNAMIC FUNCTIONS

One often encounters three terms in the scientific literature relating to surfaces: (a) the surface tension, (b) the surface energy and (c) the surface stress. All three quantities have units of energy per area (J/m²) or force per length (N/m). The term surface tension is appropriate when referring to liquids, because liquids cannot support shear stresses and atoms in the liquid can diffuse fast enough to accommodate any changes in the surface area. This is not the case for solid surfaces and solid–solid interfaces, which usually possess elastic stresses up to the melting temperature. Hence, use of the term surface tension is not clear in the case of solids, and we do not use it further. The surface energy and surface stress sufficiently define the state of all surfaces [1–6], and we refer to these quantities in this book. As we formally

derive below, the relationship among the surface energy and surface stress is that solid surfaces can change their energy in two ways:

- By increasing or decreasing the physical area of the surface; for example, by cleaving a surface or adding atoms to the surface with the arrangement of the atoms being identical to those in the bulk.
- 2. By changing the positions of atoms at a surface through elastic deformation; for example, by phenomena such as surface relaxation or reconstruction.

The first case involves simply creating more or less surface area and is independent of the nature of the surface, whereas the second case involves the detailed arrangements of atoms within a solid surface and may be thought of as the work involved in straining a unit area of surface.

Consider a large homogeneous crystalline body that contains N atoms and is surrounded by plane surfaces [7]. The energy and entropy of the solid per atom are denoted by  $E_{\rm a}$  and  $S_{\rm a}$ . The specific surface energy,  $E_{\rm s}$  (energy per unit area), is defined by the relation

$$E = NE_a + AE_s, (3.1)$$

where E is the total energy of the body and A is the surface area. Thus  $E_s$  is the excess of the total energy E that the solid has over the value  $NE_a$ , which is the value it would have if the surface were in the same thermodynamic state as the homogeneous interior. Similarly, we can write the total entropy of the solid as

$$S = NS_a + AS_s, (3.2)$$

where  $S_s$  is the specific surface entropy (entropy per unit area of surface created). The specific surface work content,  $F_s$  (energy per unit area), is defined by the equation

$$F_{s} = E_{s} - TS_{s} \tag{3.3}$$

and the specific surface free energy (energy per unit area) is defined by

$$G_{\rm s} = H_{\rm s} - TS_{\rm s},\tag{3.4}$$

where  $H_s$  is the specific surface enthalpy (that is, the heat absorbed by the system per unit surface area created). The total free energy of a system G can then be expressed as

$$G = NG_a + AG_s, (3.5)$$

similar to the total energy and entropy in Eqs. (3.1) and (3.2). We have therefore de-

fined the thermodynamic properties that are due to the presence of the surface surrounding the condensed phase.

To create a surface we have to do work on the system that involves breaking bonds and removing neighboring atoms. Under conditions of equilibrium at constant T and P, the reversible surface work dW required to increase the surface area A by an amount dA, in a one-component system, is given by

$$dW_{s(T,P)} = \gamma dA, \tag{3.6}$$

49

where the term  $\gamma$  is called the surface energy and its units are  $J/m^2$  (or N/m).

In the absence of any irreversible process, the reversible work  $dW_{s(T,P)}$  is equal to the change in the total free energy of the surface. The total surface free energy is thus equal to the specific surface free energy times the surface area

$$dW_{s(T,P)} = d(G_sA). \tag{3.7}$$

Creation of a stable interface always has a positive free energy of formation. This reluctance of a solid or liquid to form a surface defines many of the interfacial properties of condensed phases. For example, liquids tend to minimize their surface area by assuming a spherical shape. As we see shortly, solids that are near equilibrium with their own liquid or vapor form surfaces of lowest free energy at the expense of surfaces of higher free energy. Crystal faces that exhibit the closest packing of atoms tend to be the surfaces of lowest free energy and hence the most stable. As shown in later chapters, this characteristic also dominates the behavior of solid—solid interfaces and is thus very important.

As mentioned above, there are two ways of forming new surface: (a) by simply increasing the surface area or (b) by stretching the already existing surface with the number of atoms fixed and thereby altering the state of strain. Considering both possibilities, we can rewrite the right-hand side of Eq. (3.7) as

$$dW_{s(T,P)} = G_s dA + \left(\frac{\partial G_s}{\partial A}\right)_{T,P} A. \tag{3.8}$$

If we create the new surface by increasing the area, the specific surface free energy  $G_s$  is independent of the surface area so that  $(\partial G_s/\partial A)_{T,P} = 0$ , and the surface work is given by

$$dW_{s(T,P)} = G_s dA. (3.9)$$

This happens when we increase the surface area by cleavage without any atomic adjustments at the new surface for example. Comparing Eqs. (3.6) and (3.9) shows that  $\gamma = G_s$ , which means that the surface energy  $\gamma$  is equal to the specific surface free energy for a one-component system [6,7].

In the case of solids, elastic deformation of the material can lead to new surface due to strain. The elastic deformation of a solid surface can be expressed in terms of

compressive surface stress. The surface stress can be considered to act tangentially along the surface.

We defer further discussion of the surface stress until Section 4.6, except to note that when elastic and plastic surface terms are incorporated into the surface,  $\partial \gamma / \partial e_{ii}$ can be negative. In this situation, dislocations and elastic buckling of the surface can occur, which has been observed experimentally, as illustrated by the high-resolution transmission electron microscope (HRTEM) image of a {111} gold surface in Figure 3.1 [10,11].

Based on Eqs. (2.1) and (2.2), the change in the total free energy dG of a onecomponent system with the inclusion of the increase of free energy with increasing surface can be written as

$$dG = -SdT + VdP + \gamma dA. \tag{3.13}$$

51

If we differentiate Eq. (3.4) as a function of temperature, we obtain

$$\left(\frac{\partial G_{s}}{\partial T}\right)_{P} = \left(\frac{\partial \gamma}{\partial T}\right)_{P} = -S_{s},\tag{3.14}$$

where it is apparent that the surface free energy changes with temperature because of the change in entropy at the surface. Intuitively, we expect that surface atoms have more freedom of movement than atoms in the bulk and therefore a higher thermal entropy. Extra configurational entropy can also be introduced into the surface by the formation of surface vacancies (e.g., as discussed in Sec. 4.2). The surface energy of a crystal therefore is associated with a positive excess entropy, which means that  $(\partial \gamma/\partial T)_P$  is negative. Hence, as the temperature increases, the surface energy  $\gamma$  decreases, because the increasing excess entropy tends to compensate for the high excess enthalpy in Eq. (3.4), which results from the broken atomic bonds at the surface.

Because the surface energy is a quantity that can be directly measured, by measuring its temperature dependence, it should be possible to extract the excess surface entropy. Although reliable data of this type are fairly scarce, Figure 3.2 shows the variation in the surface energy of copper, silver and gold with temperature

We can define a surface stress tensor 
$$f_{ij}$$
 that relates the work associated with the variation in  $\gamma A$ , the total excess free energy of the surface due to the strain  $de_{ij}$  as

a surface elastic strain tensor  $\epsilon_{ij}$  where i,j=1,2 [2–5]. Consider a reversible process that causes a small variation in the area through an infinitesimal elastic strain de,

Since  $d(\gamma A) = \gamma dA + A d\gamma$  (Eqs. 3.7 and 3.8) and  $dA = A \delta_{ii} de_{ii}$ , where  $\delta_{ii}$  is the Kronecker delta [8], the surface stress can be expressed as

 $d(\gamma A) = A f_{ii} de_{ii}$ 

$$f_{ij} = \gamma \delta_{ij} + \frac{\partial \gamma}{\partial e_{ij}},\tag{3.11}$$

(3.10)

where  $\partial \gamma / \partial e_{ii}$  accounts for stretching of the surface and  $\partial \gamma / \partial e_{ii} = (\partial G_s / \partial A)_{TP}$  in terms of the notation in Eq. (3.8).

In contrast to the excess surface free energy y, which is a scalar, the surface stress  $f_{ii}$  is a second rank tensor. For a general surface, it can be referred to a set of principal axes such that the off-diagonal components are identically zero. In addition, the diagonal components are equal for a surface possessing a rotation axis of threefold or higher symmetry [9]. Thus, the surface stress for high-symmetry surfaces is isotropic and can be taken as a scalar quantity

$$f = \gamma + \frac{\partial \gamma}{\partial e}$$
 (3.12a)

which can also be written as

$$(f - \gamma) = \frac{\partial \gamma}{\partial e},\tag{3.12b}$$

showing that the difference between the surface stress f and the surface energy  $\gamma$  is equal to the change in surface free energy per unit change in elastic strain of the surface. Note that only when  $\partial \gamma/\partial e = 0$  is the surface stress f in Eq. (3.12a) equal to the specific surface free energy  $\gamma$ , as in the case of liquids. For most solids  $\partial \gamma / \partial e \neq 0$ . The surface stress f can be either positive or negative and is generally on the same order of magnitude as  $\gamma$ , whereas  $\gamma$  is always positive for a clean surface. The quantity  $\gamma$  is a scalar quantity, but it can also vary with the surface orientation and is therefore a scalar function of the unit vector along the surface normal (as shown in Sec. 3.4).

The physical origin of the surface stress can be qualitatively explained as follows [3]. Atoms at the surface have fewer bonds than those in the interior. If the surface atoms were not constrained to remain structurally coherent with interior atoms, they would have an equilibrium interatomic distance that is different from the bulk. As a result, the interior atoms can be considered to exert a stress on the surface. When f is positive, the surface work fdA is negative if dA is negative. This indicates that the surface could lower its energy by contracting and is under tension. Therefore, a positive f is referred to as a tensile surface stress, and a negative f is referred to as a

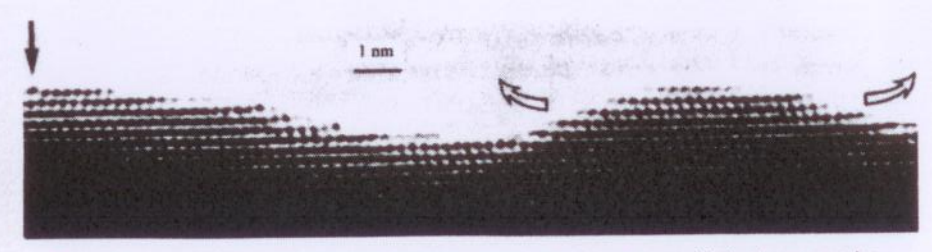


Figure 3.1. Image of a gold {111} surface buckled under surface stress. Vertical arrow marks a surface dislocation. From [10,11], reprinted with the permission of Cambridge University Press.

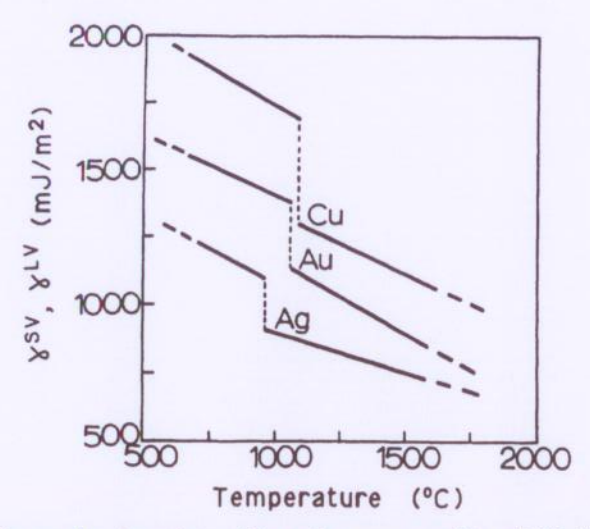


Figure 3.2. Temperature dependence of the surface energy and the solid-liquid phase transition for three f.c.c. metals. From [12].

through their melting points  $T_{\rm m}$  [12]. The symbols  $\gamma^{\rm SV}$  and  $\gamma^{\rm LV}$  are used to indicate that the solid and liquid surfaces are in equilibrium with the vapor phase, respectively. The corresponding values of  $(\partial \gamma^{\rm SV}/\partial T)_P$  obtained from these data are -0.50, -0.47 and -0.43 mJ/m<sup>2</sup>·K, respectively.

A value of about  $-0.45 \text{ mJ/m}^2 \cdot \text{K}$  for  $(\partial \gamma^{\text{SV}}/\partial T)_P$  appears to be a reasonable approximation for many solid metals. The discontinuity of approximately 25% in the surface energy at  $T_{\text{m}}$  is related to the heat of fusion and is well established [12,13]. In general, the ratio of the surface energy of the solid  $\gamma^{\text{SV}}$  to that of the liquid  $\gamma^{\text{LV}}$  is approximately 1.1 to 1.2, as mentioned earlier with respect to Table 1.1, so that surface-energy data for solids can be estimated from those of the liquids that are more abundant according to the formula

$$\gamma^{\text{SV}} \cong 1.2(\gamma^{\text{LV}})_{\text{m}} + 0.45(T_{\text{m}} - T),$$
 (3.15)

where  $(\gamma^{LV})_m$  is the liquid surface energy at the melting point,  $T_m$  is the melting temperature, and T is the temperature below the melting point of the solid.

Because the surface energy decreases with temperature, the work necessary to create more surface decreases with increasing temperature. A semiempirical equation for predicting the temperature dependence of the surface energy of liquids was proposed by van der Waals and Guggenheim [14,15] as

$$\gamma^{LV} = \gamma_0 (1 - T/T_c)^n, \tag{3.16}$$

where  $T_c$  is the critical temperature and  $\gamma_0 = \gamma^{LV}$  at 0 K. According to Eq. (3.16), the

surface energy should vanish at  $T=T_{\rm c}$  because the phases become indistinguishable and the interface between them vanishes at the critical temperature. If the exponent n is near unity, the surface energy varies linearly up to the critical temperature as illustrated in Figure 3.2. The value of n has been determined as about 1.2 for metals by experiment [12,13], indicating approximate agreement with this relationship. Illustration of the atomic structure of a liquid surface and the density as a function of temperature are shown in Figure 3.3. At the critical temperature, the surface energy approaches zero and the atoms (or molecules) in the liquid are so weakly bound that the surface definition is lost and the density of the liquid and vapor become equal. Although this illustration is for a liquid-vapor interface, it is a general picture that applies to other interfaces, including solid-vapor and some solid-solid interfaces.

## 3.2. CORRELATION OF SOLID SURFACE ENERGY WITH PHYSICAL PROPERTIES

A strong correlation exists between the surface energies of solids and their corresponding physical properties. The basis of this correlation is that the surface energy and the physical properties all depend on the strength of the interatomic bond. Atoms at a surface do not have as many nearest neighbors as those in the bulk, and therefore their energy is higher. As shown in the next section, the magnitude of the surface energy depends on the number of broken bonds associated with the surface atoms and on the strength of the broken bonds.

The following three figures show that there is a linear relationship between ex-

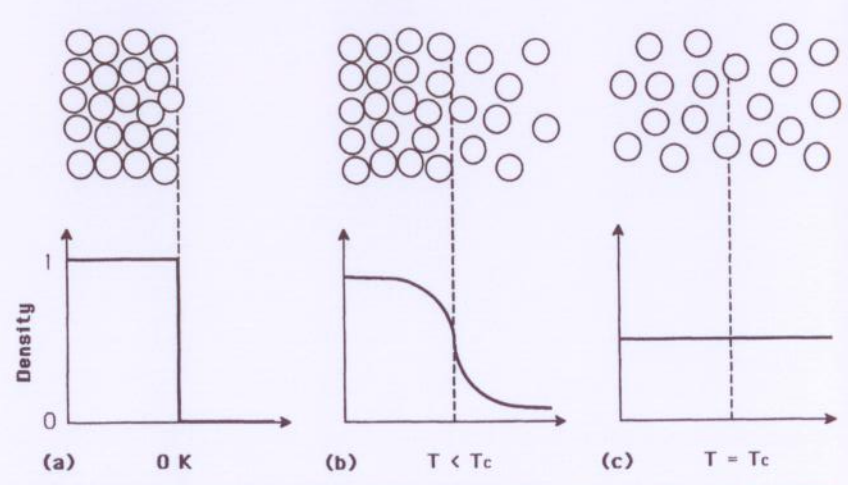


Figure 3.3. Illustration of the atomic structure of a liquid-vapor interface and the density across the interface: (a) at 0 K, (b) at  $T < T_c$ , and (c) at  $T \cong T_c$ .

perimentally measured surface energies and the heats of sublimation (Fig. 3.4), the moduli of elasticity (Fig. 3.5) and the Debye temperatures (Fig. 3.6), respectively, for a variety of metals and alloys. A similar correlation exists with the melting temperatures. Thus, to first approximation, the surface energy of a metal can be estimated from one of its physical properties such as the enthalpy of sublimation or Debye temperature using the slopes in these graphs. These properties were related to the strength of the interatomic potential  $-\epsilon_b$  in Eqs. (1.4) and (1.15). Note that the experimental surface energies in these graphs were measured near the melting point where surface stresses (Eq. 3.12) may be low but are still present.

Table 3.1 shows experimentally measured average surface energies of various solid and liquid metals, ceramics and organic liquids. It can be seen that metals generally have surface energies in the range of 1,000–2,000 mJ/m², that ionic crystals tend to be lower by a factor of approximately 2, and that the surface energies of organic liquids are generally much lower, by about two orders of magnitude. These differences become very important when we consider wetting of one material by another, a topic that is discussed in Chapter 7.

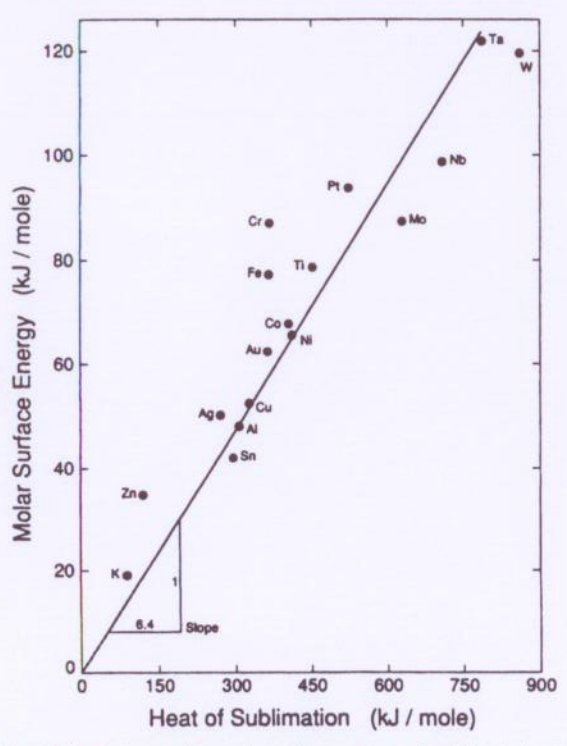


Figure 3.4. Correlation between the molar surface energy of solid metals at their melting point and the heat of sublimation. Reprinted with permission from [16].

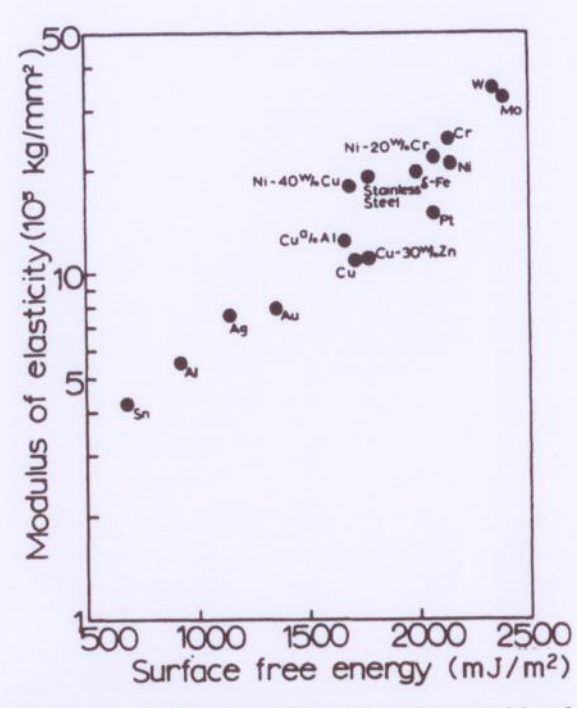


Figure 3.5. Surface energy of solid metals  $(\gamma^{\text{SV}})$  and alloys versus modulus of elasticity in tension (Young's modulus) at  $0.9T_{\text{m}}$ . From [12].

# 3.3. CALCULATION OF SURFACE ENERGY USING A NEAREST-NEIGHBOR BROKEN-BOND MODEL

For a first approximation, we can discuss the structure of solid surfaces in terms of a hard-sphere model. This is not a bad approximation given the strong  $(r^{-12})$  repulsion between atoms in metals. If the surface is parallel to a low-index crystal plane, the atomic arrangement in the plane can be assumed to be the same as in the bulk, except for perhaps a small change in lattice parameter. (The actual structure of low-index f.c.c. metal surfaces is described in a subsequent section for comparison.) Figure 3.7 shows hard-sphere models of the  $\{111\}$ ,  $\{100\}$  and  $\{110\}$  atom planes in f.c.c. metals. Except for the close-packed  $\{111\}$  plane, the density of atoms in f.c.c. planes generally decreases as the  $\{hkl\}$  Miller indices of the plane increase. The surface energy originates because atoms in the surface plane are missing some of their neighbors and therefore possess a higher energy than those in the bulk (i.e., an excess energy due to broken bonds).

We can calculate the surface energy of a pure solid f.c.c. metal using a simple nearest-neighbor broken-bond model of the surface. The assumptions used in this model are the following:

Table 3.1. Average surface energies of selected solids and liquids at the indicated temperatures

Material	$\gamma (mJ/m^2)$	T (°C)	
W (solid)	2900		
Nb (solid)	2100	2250	
Au (solid)	1410	1027	
Au (liquid)	1140	1338	
Ag (solid)	1140	907	
Ag (liquid)	879	1100	
Fe(solid)	2150	1400	
Fe (liquid)	1880	1535	
Pt (solid)	2340	1311	
Cu (solid)	1670	1047	
Cu (liquid)	1300	1535	
Ni (solid)	1850	1250	
Hg (liquid)	487	16.5	
LiF (solid)	340	-195	
NaCl (solid)	227	25	
KCl (solid)	110	25	
MgO (solid)	1200	25	
CaF <sub>2</sub> (solid)	450	-195	
BaF <sub>2</sub> (solid)	280	-195	
He (liquid)	0.31	-270.5	
N <sub>2</sub> (liquid)	9.71	-195	
Ethanol (liquid)	22.75	20	
Water	72.75	20	
Benzene	28.88	20	
r-Octane	21.80	20	
Carbon tetrachloride	26.95	20	
Bromine	41.5	20	
Acetic acid	27.8	20	
Benzaldehyde	15.5	20	
Vitrobenzene	25.2	20	

Source: From [7].

- 1. Each atom is bonded to z nearest neighbors (coordination number) and only the energies of the nearest neighbors are considered.
- 2. Each bond has an energy  $-\epsilon_b$  that is not a function of temperature.
- 3. The energy is equal to the heat of sublimation  $\Delta H_s$  per mole divided by the total number of bonds, as in Eq. (1.4).
- 4. The enthalpies and internal energies are equal.

Consider the  $\{111\}$  surface in Figure 3.7a, for example. We see that, when an f.c.c. crystal with z=12 is separated on a  $\{111\}$  plane, there are six nearest neigh-

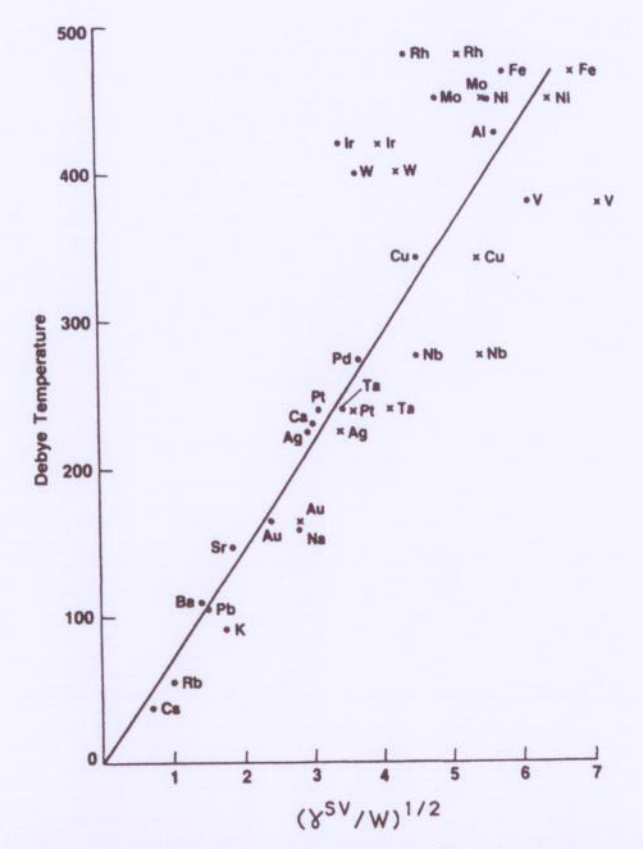


**Figure 3.6.** Debye temperature versus  $(\gamma^{SV}/W)^{1/2}$ , where  $\gamma^{SV}$  is the surface energy (mJ/m²) and W is the atomic weight. The straight line represents a theoretically predicted relationship for cubic solids. From [17].

bors in the plane, three atoms above the plane and three below. As a result, three bonds are broken for each surface atom when the crystal is separated to form two  $\{111\}$  planes. Thus, every surface atom has an excess internal energy of  $3\epsilon_b/2$  over the atoms in the bulk. Consequently, the energy of a  $\{111\}$  surface is given by

$$E_{\rm s} = \frac{3\epsilon_{\rm b}}{2} = \frac{3\Delta H_{\rm s}}{12N_{\rm A}} = \frac{\Delta H_{\rm s}}{4N_{\rm A}} \tag{3.17}$$

in joules per atom. If there are  $N_{s\{hkl\}}$  atoms/m<sup>2</sup> on the  $\{hkl\}$  surface and there are no surfaces strains, then the surface energy  $\gamma_{\{hkl\}}^{SV}$  is given as

$$\gamma_{\{111\}}^{SV} = N_{s\{111\}} E_s = N_{s\{111\}} \Delta H_s / 4N_A \tag{3.18a}$$

in joules per square meter. Similarly, for a {100} surface

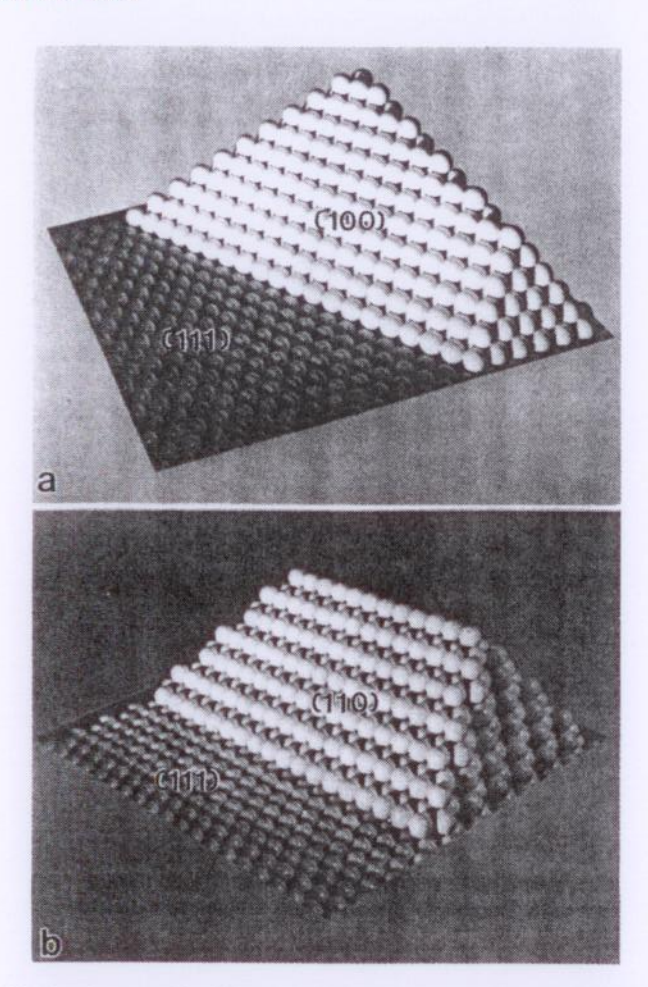


Figure 3.7. Hard-sphere models of (a) the {111} and {100}, and (b) the {110} crystal surfaces for an f.c.c. metal based on a stacking of {111} atom planes. From [18].

$$\gamma_{(100)}^{SV} = N_{s(100)} \Delta H_s / 3N_A \tag{3.18b}$$

and, for a {110} surface

$$\gamma_{\{110\}}^{SV} = N_{s\{110\}} \Delta H_{s}/2N_{A}. \tag{3.18c}$$

Note that it is difficult to find the sixth broken bond at the {110} surface, because it is associated with the second layer of atoms below the surface. (This point is illustrated in Problem 4.10.) Comparing Eqs. (3.18) immediately shows that the surface energy of a {110} surface is higher than that of a {100} surface, which is higher

than that of a  $\{111\}$  surface, independent of the magnitude of the bond energy. This same broken-bond approach can be used to estimate the energy of any  $\{hkl\}$  crystal surface.

The calculations above are for specific crystal planes. When  $\gamma^{SV}$  is measured experimentally for a material (as in Table 3.1 for example), it is often an average value obtained over many different crystal planes. It is difficult to calculate an average value of  $\gamma^{SV}$  from the nearest-neighbor broken-bond model because the average number of broken bonds and surface area per atom are not known. An alternative expression for calculating the average surface energy of metals that takes into account the size of the atoms and thus the energy per unit surface [19] is given by

$$\gamma^{SV} = C_1 \Delta H_s / V_m^{2/3}, \tag{3.19}$$

where  $V_{\rm m}$  is the molar volume of the metal and  $C_1$  is a proportionality constant  $(6N_{\rm A}^{1/3})^{-1}$  equal to  $2\times10^{-9}$  mol<sup>1/3</sup> when  $\gamma^{\rm SV}$  is in mJ/m<sup>2</sup> (or 20 when  $\gamma^{\rm SV}$  is expressed in kJ/cm<sup>2</sup>),  $\Delta H_{\rm s}$  is in kJ/mol and  $V_{\rm m}^{2/3}$  is in m<sup>2</sup>/mol<sup>2/3</sup>. This relationship is illustrated in Figure 3.8 and it is based on Miedema's semiempirical model of alloy formation [20]. The individual data points for  $\gamma^{\rm SV}$  in Figure 3.8 are given in Appendix C.

Table 3.2 compares the {111}, {100} and {110} surface energies calculated according to Eq. (3.18), with average values obtained experimentally from Table 3.1, with values calculated from Eq. 3.19 and using the embedded-atom method (EAM) [21] described in Section 1.3. Note that the results of both the nearest-neighbor bro-

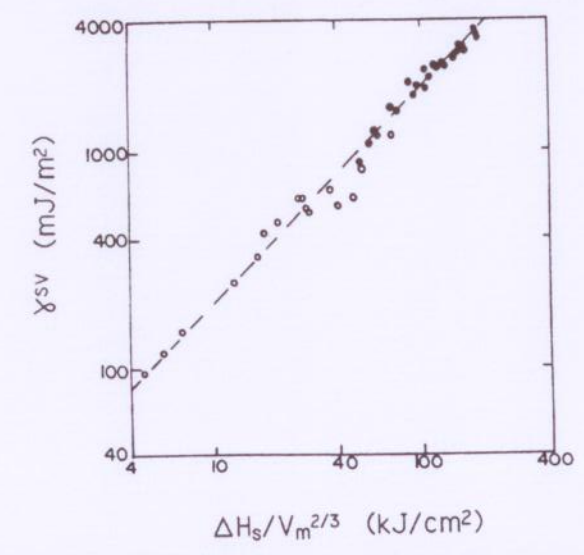


Figure 3.8. Illustration of the linear relationship between the surface energy and heat of sublimation per unit molar surface for solid metals at T = 0 K. Open circles correspond to nontransition metals and filled circles to transition metals. In this plot,  $C_1 = 20$  because the units are kJ/cm<sup>2</sup>. From [19].

Table 3.2. Surface energies of copper calculated according to Eq. (3.18) compared to values obtained by embedded-atom method calculations at 0 K, from Eq. (3.19), and experimentally determined average values near  $T_{\rm m}$ 

Element	{111}	{100}	{110}	Experiment	Eq. (3.19)
Cu (Eq. 3.18)	1240	1430	1520	_	_
Cu (EAM)	1170	1280	1400	1670	1799
Ag (EAM)	620	705	770	1140	1195
Au (EAM)	790	918	980	1410	1537

\*Values for Au and Ag are also included for comparison and all units are in mJ/m2.

Source: Embedded-atom method calculations from [21]. Experimentally determined average values from [7].

ken-bond model and EAM calculations show the same trend in energies among the metals, although the EAM calculations at 0 K are consistently lower. The average experimental values are generally higher than either calculational method and compare favorably with the results of Eq. (3.19), although the latter are somewhat higher. These results indicate that the simple nearest-neighbor bond model is able to account qualitatively for the behavior of the surface energy as a function of orientation in f.c.c. metals and provide a reasonable estimate of the magnitude of the surface energy, accurate to within maybe 10%. It must be remembered that the nearest-neighbor model is only approximate, and, therefore, these are quite satisfying results. [Note: Many of the surface energy data in the literature are given in units of ergs/cm². Fortunately, this easily converts since 1 erg/cm² = 1 mJ/m² (Appendix A).]

## 3.4. THE $\gamma$ PLOT

It is clear from the previous section that the surface energy of a solid varies as a function of the crystal surface orientation. In many cases, we need to know how the surface energy varies for all possible surface orientations, and we also need a convenient method to display calculated and experimental surface-energy data for comparison. This can be accomplished using a so-called  $\gamma$  plot, where the surface energy is plotted as a function of surface oriention (pole normals) on a stereographic projection. Due to the high symmetry of cubic crystals, the entire orientation dependence can be displayed on the stereographic triangle bounded by the {111}, {100} and {110} poles, as illustrated in Figure 3.9.

Nicholas et al. [22,23] have calculated  $\gamma^{SV}$  plots for f.c.c. and b.c.c. metals using an unrelaxed nearest-neighbor broken-bond model and interaction potentials of various types, including the Lennard-Jones 6-12 potential discussed in Chapter 1. They also compared the effects of using first-, second- and higher-nearest-neighbor interactions in the calculations. Their equation for the surface energy  $\gamma^{SV}_{\{hkl\}}$  as a function of orientation is

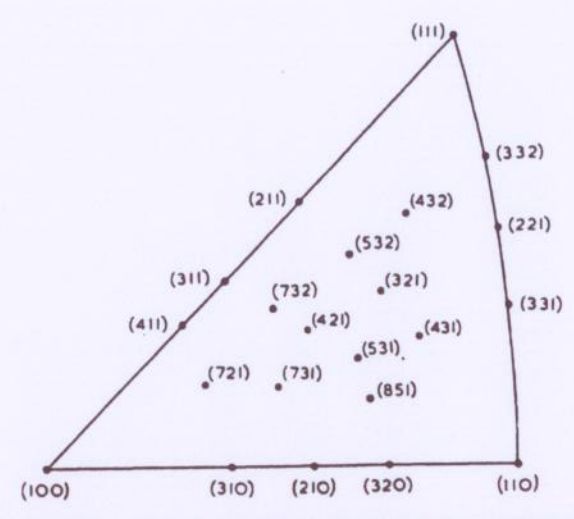
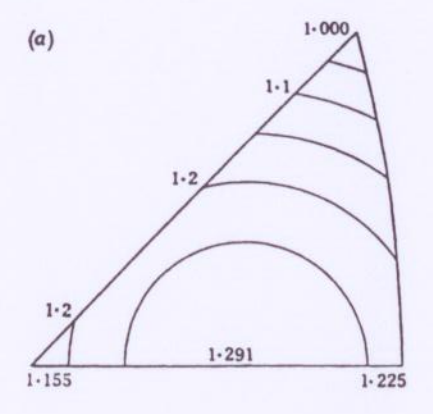


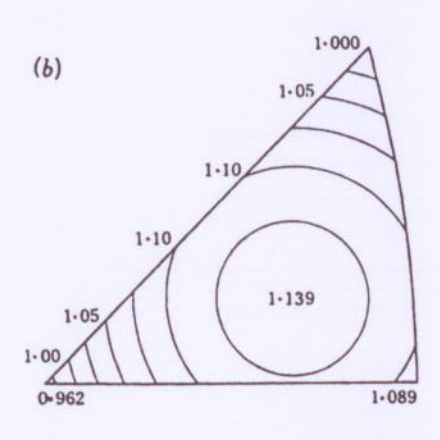
Figure 3.9. Stereographic plot of the normals to the surfaces for a cubic structure. From [18].

$$\gamma_{\{hkl\}}^{SV} = \frac{d_{\{hkl\}}}{V_{a}} \sum \left(\frac{-\epsilon_{b}}{2}\right) (\mathbf{n}_{\{hkl\}} \cdot \mathbf{u}_{i}), \tag{3.20}$$

where  $V_a$  is the volume of the crystal per atom with an associated  $\mathbf{u}$  bond (for an f.c.c. crystal,  $V_a$  is just the volume of a primitive unit cell of the structure since every atom is associated with a  $\mathbf{u}$  bond),  $\mathbf{n}_{\{hkl\}}$  is the normal vector of a plane with  $\{hkl\}$  indices, where h, k and l are the components of  $\mathbf{n}_{\{hkl\}}$  when referred to the corresponding unit cell of the reciprocal lattice, and interplanar spacing  $d_{\{hkl\}} = 1/|\mathbf{n}_{\{hkl\}}|$ , and  $\mathbf{u}_i$  is a unit vector which specifies the direction of the ith crystal bond about the atoms. The quantity  $d_{\{hkl\}}/V_a$  represents the area of the (primitive) unit cell of surface on the  $\{hkl\}$  plane. The summation is performed over all bonds with a positive value of  $\mathbf{n}_{\{hkl\}}$   $\mathbf{u}_i$  (i.e., those bonds pointing out of the  $\{hkl\}$  surface plane).

Results from three of their calculations including nearest-neighbor, second-nearest-neighbor and many-neighbor interactions are shown in Figures 3.10a, b and c, respectively. In Figure 3.10a, the surface energies of the  $\{111\}$ ,  $\{100\}$  and  $\{110\}$  surfaces scale as in our broken-bond calculations in the previous section. In addition, the maximum surface energy occurs for the  $\{210\}$  plane. The difference in surface energy between the  $\{111\}$  and  $\{210\}$  planes is about 29%. Two significant differences occur when second nearest neighbors are included in the calculations. As shown in Figure 3.10b, the maximum surface energy shifts toward the  $\{211\}$  pole and the surface energy of the  $\{100\}$  plane becomes less than that of  $\{111\}$ . When the calculations include nearest neighbors up to approximately 22 times the interactomic distance, the  $\{111\}$  surface again has the lowest surface energy and the maximum anisotropy is only approximately 12%, as shown in the  $\gamma^{\rm SV}$  plot in Figure 3.10c.





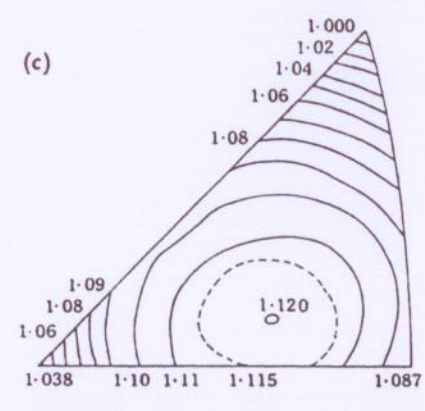


Figure 3.10. Theoretical contour plots of solid surface energy for an f.c.c. crystal when (a) nearest-neighbor, (b) second-nearest-neighbor and (c) many-neighbor interactions are considered. From [23].

Figure 3.11 shows experimental  $\gamma^{\rm SV}$  plots for the surface energy of copper obtained from grain boundary grooving experiments at three different temperatures approaching the melting point [24]. These data show that the surface energies of the {111}, {100} and {110} surfaces generally increase in this order, in agreement with the plots in Figures 3.10a and c, but the differences between them are much smaller, and there is not a pronounced minimum at {110}. In contrast to the calculations above, the maximum difference in surface energy at the lowest temperature of 830°C is only 3.5% and this difference decreases to 1.7% at 1030°C. These data indicate that the broken-bond model at 0 K overestimates the magnitude of the anisotropy of the surface energy, particularly in the case when only nearest neighbors are included in the calculations. Qualitatively, the form of the  $\gamma^{\rm SV}$  plots at the lower temperatures is similar to those shown in Figure 3.10, so that the nearest-neighbor bond model is able to offer insight into the variation of surface energy with orientation.

### 3.5. THE WULFF PLOT AND WULFF CONSTRUCTION

#### 3.5.1. Wulff Plot

Another useful way to plot the variation in  $\gamma^{SV}$  as a function of orientation is accomplished using a Wulff plot, in which a radius vector  $\mathbf{r}_{\{hkl\}}$  represents the orientation of the surface (i.e., the direction of the surface normal  $\mathbf{n}_{\{hkl\}}$ , and the length of  $\mathbf{r}$  is given by the magnitude of the surface energy  $\gamma^{SV}\mathbf{n}_{\{hkl\}}$  so that  $\mathbf{r} = \gamma^{SV}\mathbf{n}_{\{hkl\}}(\mathbf{n}_{\{hkl\}})$ . We only consider two-dimensional Wulff plots, but the ideas apply directly to three-dimensional plots as well.

A two-dimensional section along a  $<1\overline{10}>$  direction of the Wulff plot of an f.c.c. crystal is shown schematically in Figure 3.12a. The Wulff plot has the same symmetries as the crystal and one quadrant is sufficient to specify the entire plot in Figure 3.12a [25]. Thus, the variation in  $\gamma^{SV}$  in moving along the Wulff plot may be thought of as lines of constant surface energy in the stereographic triangle as depicted in the previous  $\gamma^{SV}$  plots. There are local minima in the surface energy along the Wulff plot, which are often referred to in the literature as cusps. The surfaces corresponding to cusp orientations (like {111}) are called singular.

### 3.5.2. Wulff Construction

In this section, we examine the connection that exists between crystal morphology and the variation of  $\gamma$  with orientation. This important connection occurs not only for solid-vapor interfaces but also for all of the interfaces that we consider in this book. We first look at it from a thermodynamic or phenomenological viewpoint, and, in the next section on the terrace-ledge-kink description, we examine the same relationship on an atomistic level.

Consider a one-component system in which there are two phases  $\alpha$  and  $\beta$  separated by an interface as sketched in Figure 3.13. The  $\alpha$  phase is a solid and the  $\beta$ 

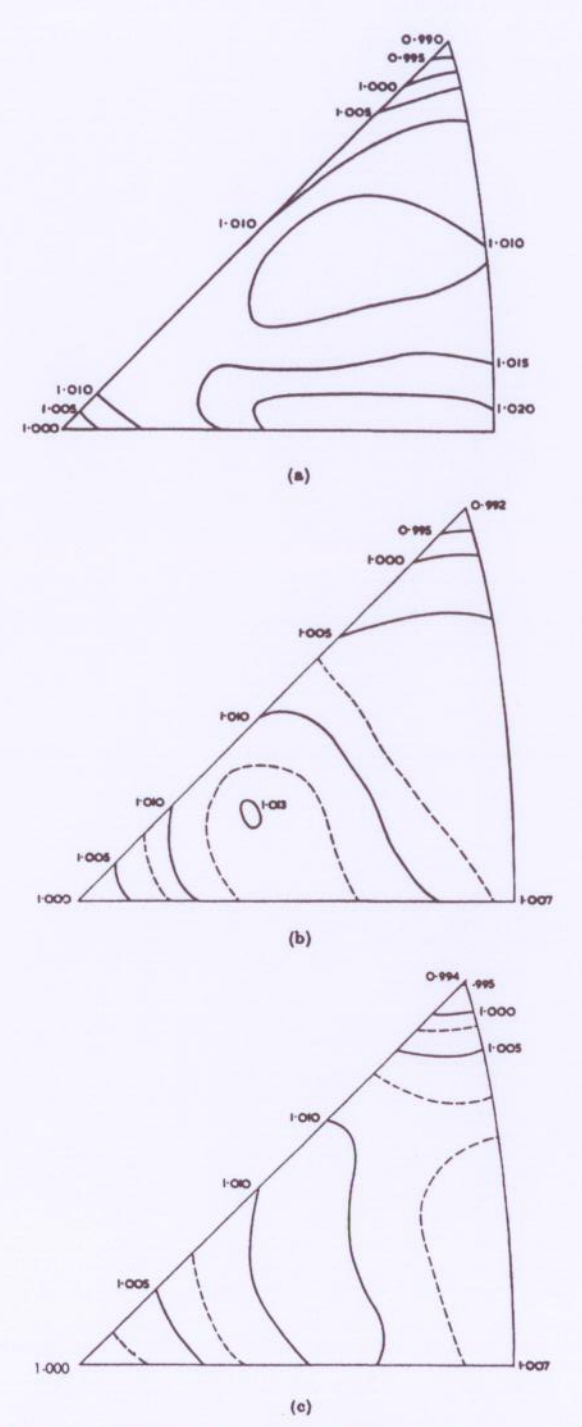
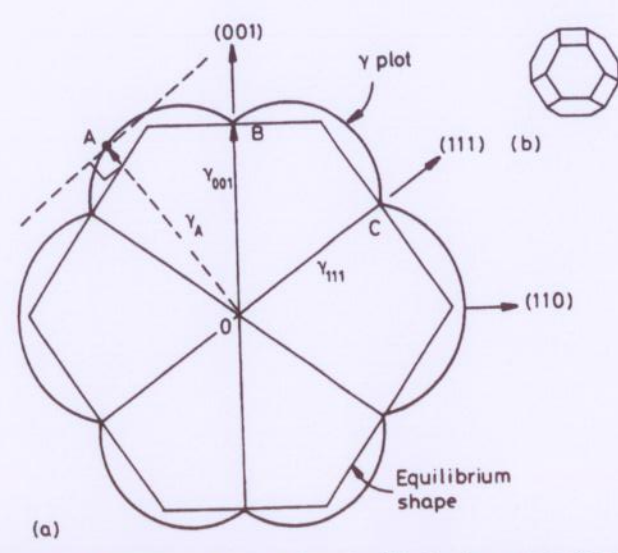


Figure 3.11. Relative  $\gamma^{SV}$  plots for copper normalized to make  $\gamma^{SV}_{(100)} = 1$  for (a) 827°C, (b) 927°C and (c) 1027°C. Reprinted with permission from [24] by Figure 1 and Conformalized to make  $\gamma^{SV}_{(100)} = 1$  for (a) 827°C, (b)



**Figure 3.12.** (a) Two-dimensional section of a polar plot of surface energy for an f.c.c. crystal oriented along <110>. The equilibrium shape of the crystal can be derived from the Wulff plot as illustrated in (b). From [25].

phase could be a vapor, liquid, or solid. We would like to know the equilibrium shape of the interface. If we assume that the  $\alpha$  and  $\beta$  phases have their equilibrium volumes and can only change their shape, then the condition of minimum free energy [26] is given by

$$\int \gamma(\mathbf{n}) dA = \text{minimum}, \tag{3.21}$$

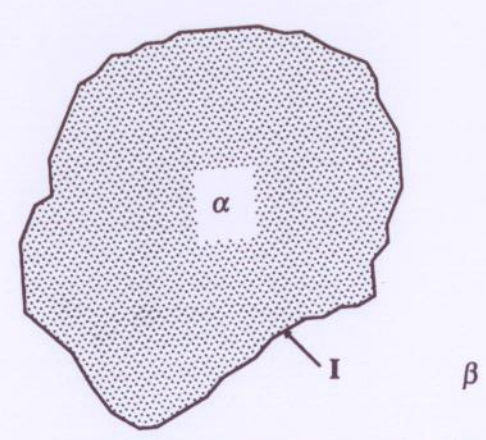


Figure 3.13. A particle of  $\alpha$  phase separated from  $\beta$  phase by an interface labeled I.

67

where the integral is taken over the interface I with normal vector n. For interfaces between simple liquids where  $\gamma$  is independent of orientation, it is clear that the condition of equilibrium is one of minimum surface area so that the equilibrium shape is a sphere. There is experimental evidence that solids also approach this condition at high temperature. However, when there is appreciable variation of  $\gamma$  with orientation as we have seen in the previous sections, the equilibrium shape will be a polyhedron with surfaces of low y being preferentially exposed (as in Figure 3.12b).

We can determine the equilibrium shape of the particle from the Wulff plot by a procedure known as the Wulff construction [26]. Although this construction allows one to determine the equilibrium crystal shape from the Wulff plot, it is not usually possible to construct a unique  $\gamma$  plot from the equilibrium crystal shape. The procedure for the Wulff construction is as follows:

- 1. Draw radius vectors from the origin to intersect the Wulff plot, as illustrated by OA in Figure 3.12a.
- 2. Construct lines (planes in three dimensions) normal to the radius vector passing through the point of intersection (dashed line perpendicular to OA).
- 3. The figure formed by the inner envelope of all these perpendiculars is the equilibrium shape, labeled in Figure 3.12a.

Therefore, when the Wulff plot contains sharp cusps, the equilibrium crystal shape is a polyhedron where the width of the crystal facets is inversely proportional to their surface energy (i.e., the largest facets have the lowest surface energy). This is illustrated by the equilibrium crystal shape shown in Figure 3.12b.

It is possible to construct several other types of  $\gamma$  plots that have some utility when considering faceting of crystal surfaces. Faceting occurs when an initially flat surface of arbitrary orientation breaks up into a hill-and-valley structure composed of portions of two or more facets that are generally low-energy (low-index) planes. A flat surface present in the equilibrium shape of the Wulff diagram is stable, whereas surfaces of other orientations are unstable and will exhibit faceting (i.e., they will break down into certain flat crystal surfaces, if kinetically feasible). Hirth [27] discusses the other types of  $\gamma$  plots (including the  $\Gamma$ ,  $\gamma^{-1}$  and  $\Gamma^{-1}$  plots) and we only consider the  $\Gamma$  plot below.

The  $\Gamma$  plot is the locus of points intersecting the radius vector from the origin and perpendicular to the radius vector that lies as far as possible from the origin while still maintaining at least one point of contact with the equilibrium shape. This plot is illustrated for a cubic crystal viewed along [001] in Figure 3.14. Any orientation for which the Wulff plot ( $\gamma$  plot) lies further from the origin than the  $\Gamma$  plot is unstable with respect to faceting, and the reduction in surface energy accompanying faceting is given by the difference between the  $\gamma$  and  $\Gamma$  values at that orientation. Note that the  $\Gamma$  plot is the minimum-valued  $\gamma$  plot that will reproduce the given equilibrium shape.

The equilibrium shape and surface energy anisotropy of crystals can be determined experimentally by annealing small single crystals in ultrahigh vacuum and

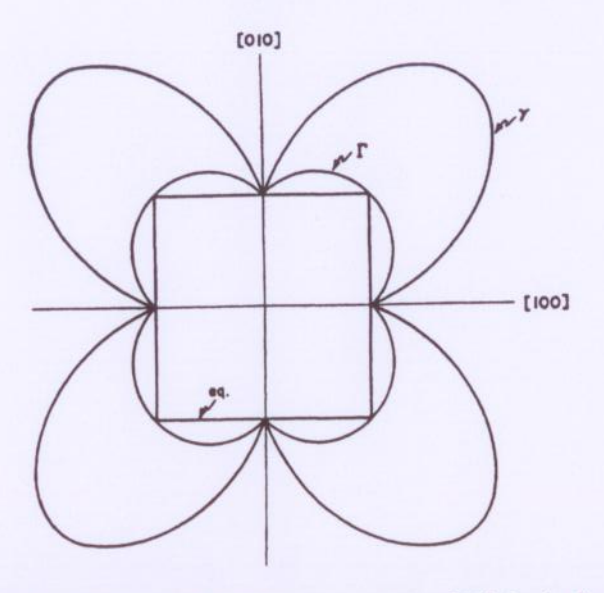


Figure 3.14. Two-dimensional polar plot for a cubic crystal along [001] showing the  $\gamma$  plot,  $\Gamma^{-1}$ plot and the equilibrium shape. From [27].

observing the shape of a crystal and the size of its facets as a function of temperature. Similar experiments are also quite useful for quantifying surface segregation as discussed in a later section. Heyraud and Metois [28,29] have performed these types of measurements for a variety of metals including f.c.c. lead and gold on graphite. Lead and gold are particularly good metals to study, because they have negligible solubility for carbon (from the substrate) and are relatively inert.

Figure 3.15 shows a scanning electron microscope image of an annealed lead particle on graphite. The <111> and <100> surface orientations are indicated on the figure, and the crystal is clearly faceted along these planes. The ratio of the widths of the facets is equal to the ratio of their surface energies. These and other facets were measured as a function of temperature in the range of 200°C to 300°C and the ratios of the surface energies as a function of temperature are shown in Figure 3.16.

The data in Figure 3.16 show that the maximum-surface-energy anisotropy at 200°C is approximately 6% along <113> and <110> and the anisotropy between <111> and <100> is less than 2%. When similar gold crystals were annealed at 1000°C the maximum-surface-energy anisotropy was 3.4% and the anisotropy between <111> and <100> was only 1.9% [28]. Both sets of results are similar to the experimental data for copper in Figure 3.11 and earlier studies of gold [30], again indicating that the previous broken-bond model overestimates the anisotropy. These data appear to be typical for f.c.c. metals.

It is also clear from Figure 3.16 that the surface energy anisotropy is temperature dependent and that it decreases as the temperature increases. The most important

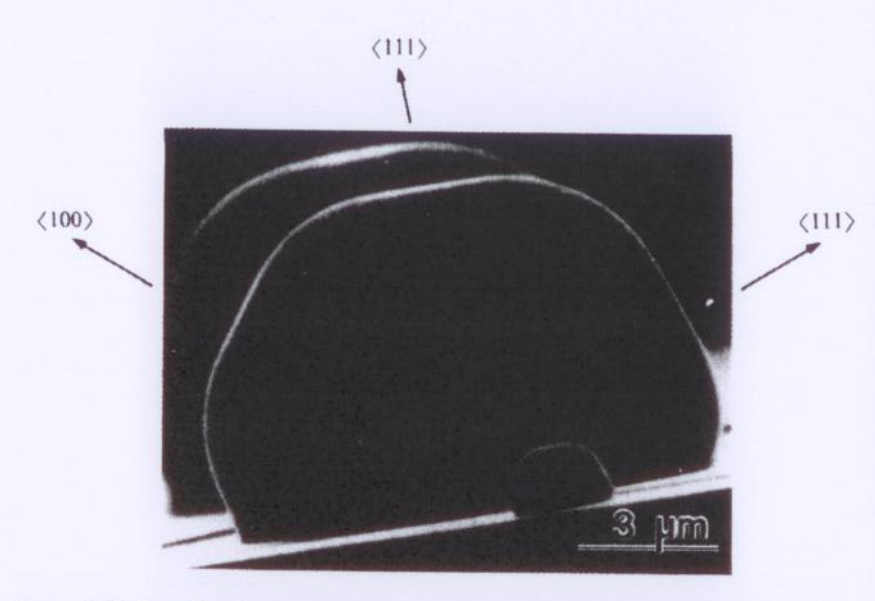
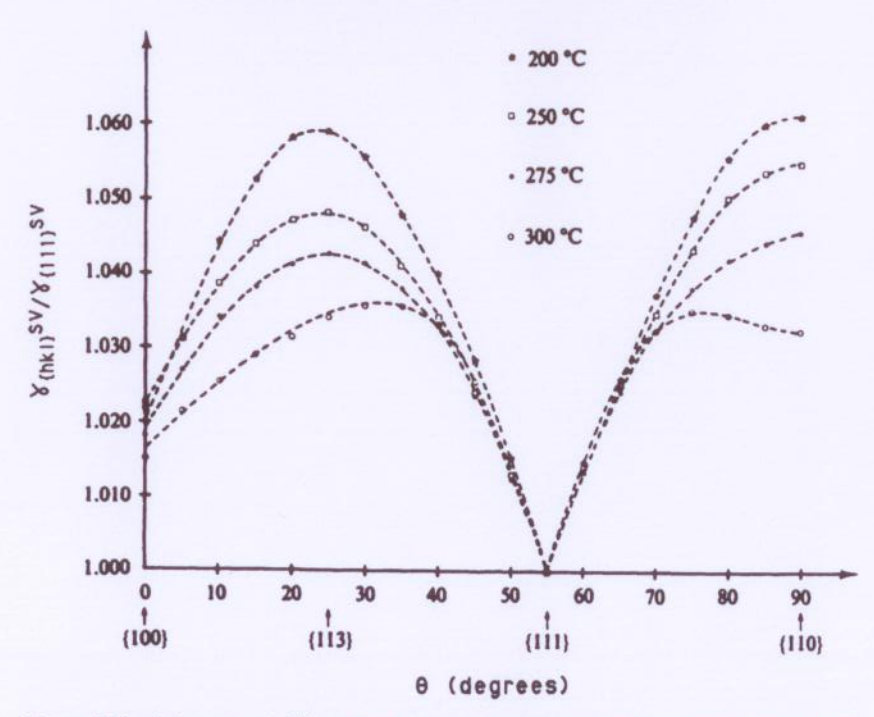


Figure 3.15. Scanning electron micrograph of a lead crystal at 200°C. From [10,29] reprinted with the permission of Cambridge University Press.



**Figure 3.16.** Anisotropy of  $\gamma_{M_0}^{\infty}$  relative to {111} for lead as a function of temperature. From [10,29] reprinted with the permission of Cambridge University Press.

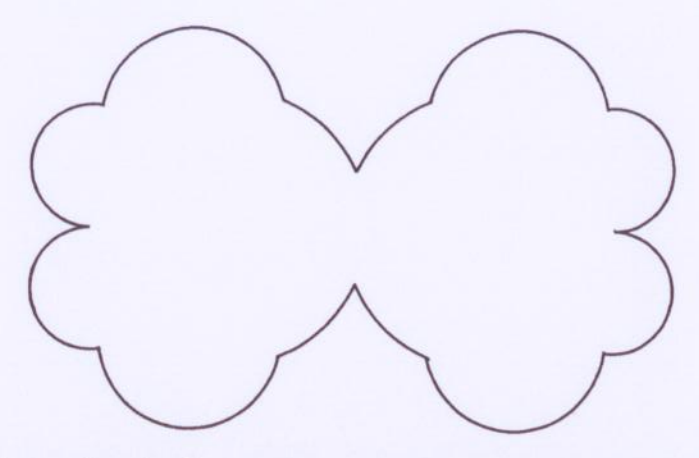
decrease occurs around the higher index <113> and <110> directions in the <110> zone and around the <120> direction in the <100> zone [29]. Note that a decrease in surface energy with increasing temperature corresponds to a positive value of surface entropy, as discussed with reference to Eq. (3.14). Because there was dispersion in the data, it was difficult to draw conclusions about the variation in the ratio  $\gamma_{\{100\}}^{SV}/\gamma_{\{111\}}^{SV}$ , but the results indicated that the ratio decreased as the temperature was raised. Lastly, the ratio  $\gamma_{\{hkl\}}^{SV}/\gamma_{\{111\}}^{SV}$  around the <111> direction seemed to be almost temperature independent.

To understand the temperature dependence of the surface energy, we need to examine the atomic structure of surfaces in greater detail. This is done in the next chapter on the terrace-ledge-kink model of surface structure. Before we move on, it is worth noting that the Wulff construction developed with regard to Figure 3.12 applies to all types of interfaces, not just to solid-vapor interfaces as emphasized in this section. We use the same construction to examine the equilibrium shapes of precipitates embedded in a matrix in Part IV, for example.

#### **PROBLEMS**

- 3.1. Starting with the definition of strain  $e = (A A_0)/A_0$ , where  $A_0$  is the initial area and A is the final area, show that de = dA/A, and hence, that  $(\partial G_S/\partial A)_{T,P} = (\partial \gamma/\partial e)_{T,P}$ .
- 3.2. Starting with Eqs. (2.1) and (2.2) and including the increase of free energy with increasing surface area, derive Eq. (3.13).
- 3.3. For an f.c.c. metal, determine the ratio  $\gamma_{\{111\}}^{SV}/\gamma_{\{100\}}^{SV}$  of the surface energies on the  $\{111\}$  and  $\{100\}$  surfaces considering both the first and second nearest-neighbor bond energies and assuming that the second nearest-neighbor bond energy equals one-quarter of the first nearest-neighbor energy.
- 3.4. (a) Assume that the atoms in a solid can be described as cubes with volume V. Show that the surface area per atom is  $6(V/N_A)^{2/3}$  and determine  $C_1$  in Eq. (3.19).
  - (b) Use Eq. (3.19) to calculate the average surface energies of copper, silver and gold and compare your results with the experimental results given in Table 3.2.
- 3.5. For f.c.c. copper with a density of 8.93 g/cm³ and an atomic mass of 63.55, determine the atomic density and lattice parameter α. Using values from tables in the text determine the solid-vapor surface energy and heat of sublimation in terms of eV/atom for the {100} surface.
- 3.6. Use Eq. (3.16) to plot  $\gamma^{SV}$  of copper from 0 to 1600 K. Compare your results with Eq. (3.15), given that  $(\gamma^{LV})_m = 1280 \text{ mJ/m}^2$  for copper.
- 3.7. Given the  $\gamma^{\text{SV}}$  plot below, use the Wulff construction to find the equilibrium shape of the crystal.



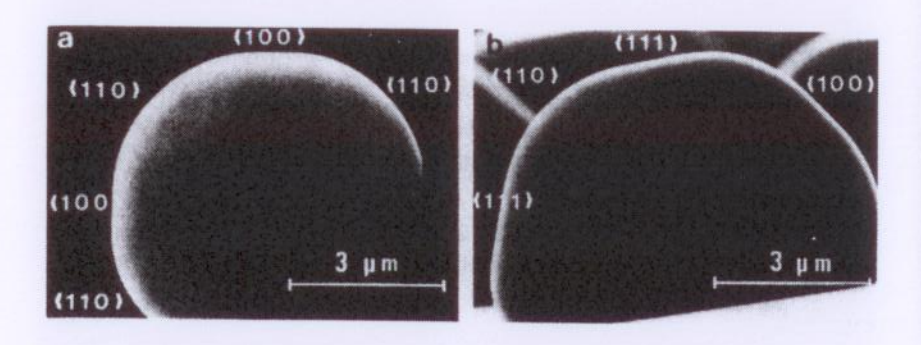


3.8. If a two-dimensional rectangular crystal is bounded by sides of lengths  $l_1$  and  $l_2$ , show by differentiation that the equilibrium shape is given by

$$\frac{l_1}{l_2} = \frac{\gamma_2^{\text{SV}}}{\gamma_1^{\text{SV}}},$$

where  $\gamma_1^{SV}$  and  $\gamma_2^{SV}$  are the surface energies of sides  $l_1$  and  $l_2$ , respectively. (The area of the crystal  $l_1 l_2$  is constant.)

3.9. The figure below (from [29]) shows two palladium particles on a graphite substrate viewed along (a) <100> and (b) <110>.



- (a) Locate the origin (Wulff point) in both figures.
- (b) Determine the ratio of the surface energy anisotropy for the {100} and {110} surfaces relative to the {111} surface by measuring the lengths of vectors from the origin according to the construction in Figure 3.12.
- (c) Compare the ratio γ<sup>SV</sup><sub>(100)</sub>/γ<sup>SV</sup><sub>(111)</sub> determined in part b with the same ratio determined by comparing the lengths of the {100} and {111} facets, and by comparing the angular width of these facets with respect to the origin. How do your measurements compare?

# SURFACE STRUCTURE

### 4.1. TERRACE-LEDGE-KINK MODEL OF SURFACES

It is useful to be able to visualize the atomic structures of surfaces and interfaces, because many important phenomena such as the mechanisms and kinetics of crystal nucleation and growth, adsorption and segregation to surfaces and even the definition of the surface depend directly on the atomic structure and atomic level defects present at these interfaces. In this section, we develop an atomic description of crystal surfaces, which we use to further understand the reason for cusps at certain crystallographic orientations in the Wulff plot and to quantify phenomena such as surface roughening (shown schematically in Figure 3.3, but only discussed in a qualitative way). Again, it is important to remember that we are concerned with solid—vapor interfaces (surfaces) in this chapter, but the ideas developed for the terrace-ledge-kink model here are equally applicable to solid—liquid and solid—solid interfaces as we shall see later.

When we considered the formation of an  $\{hkl\}$  surface using the broken-bond model in Chapter 3, we imagined that we created the surface by removing all of the atoms whose centers lay on one side of a mathematical dividing plane with this orientation located within the crystal. Since no atomic relaxations or rearrangements were allowed to occur, the surface was ideal and there was no surface stress. This led to atomic surfaces such as those shown in Figure 3.7. (An atlas of such surfaces for f.c.c. and b.c.c. crystals has been published by Nicholas [18]. This is a useful reference for visualizing various  $\{hkl\}$  surfaces.) The  $\{100\}$  and  $\{111\}$  surfaces shown in Figure 3.7a are atomically smooth and are referred to as singular, because singularities or cusps often occur in the  $\gamma^{SV}$  plot at these orientations.

A surface that is only slightly different in orientation from one that is atomically smooth consists mainly of flat regions called terraces with a system of widely spaced atomic steps or ledges. Such a surface is called vicinal. Figure 4.1a shows a vicinal surface on an f.c.c. crystal that makes an angle of approximately 11° with re-